Article

Cell Reports

Fcμ receptor as a Costimulatory Molecule for T Cells

Graphical Abstract

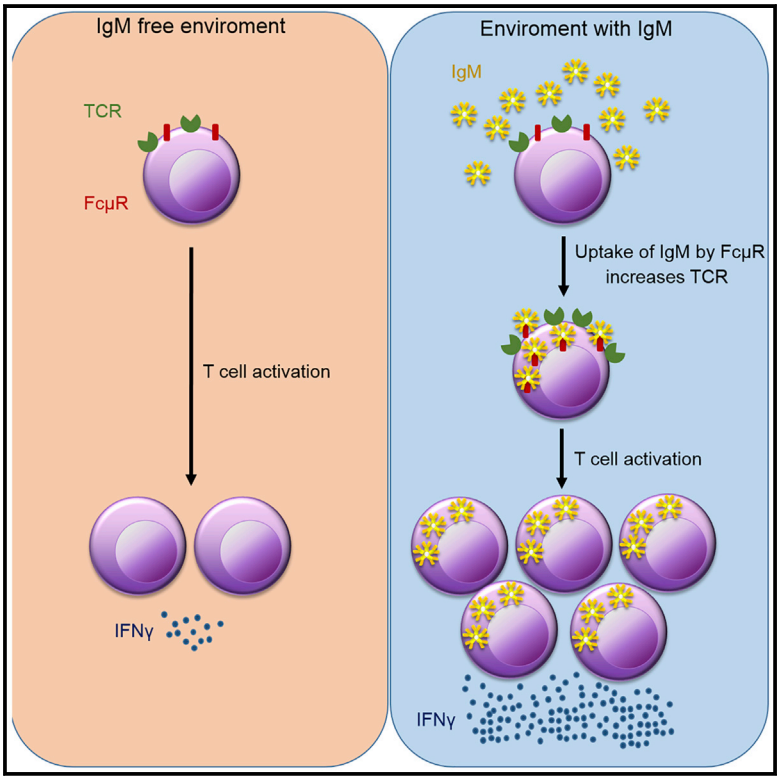

Authors

Andreas Meryk, Luca Pangrazzi, Magdalena Hagen, ..., Mikko Hurme, Klemens Trieb, Beatrix Grubeck-Loebenstein

Correspondence

andreas.meryk@uibk.ac.at

In Brief

Meryk et al. demonstrate that uptake of IgM mediated by FcμR expressed on T cells increases the surface expression of TCR and costimulatory molecules to facilitate T cell activation, particularly when antigen concentrations are low. Consequently, FcμR increases TCR signaling, proliferation, and cytokine release.

Highlights

- FcμR is expressed by T cells to ensure persistent IgM uptake
- Intracellular accumulation of IgM enhances surface T cell receptor expression
- T cell effector functions are boosted by FcμR-mediated accumulation of IgM
- Methylation of *FCMR* gene is associated with decreased protein expression in old age

Meryk et al., 2019, Cell Reports *26*, 2681–2691
March 5, 2019
https://doi.org/10.1016/j.celrep.2019.02.024

CellPress

Cell Reports
Article

Fcμ receptor as a Costimulatory Molecule for T Cells

Andreas Meryk,[1,6,7,*] Luca Pangrazzi,[1,6] Magdalena Hagen,[1,6] Florian Hatzmann,[1] Brigitte Jenewein,[1] Bojana Jakic,[2] Natascha Hermann-Kleiter,[2] Gottfried Baier,[2] Juulia Jylhävä,[3] Mikko Hurme,[4] Klemens Trieb,[5] and Beatrix Grubeck-Loebenstein[1]

[1]Department of Immunology, Institute for Biomedical Aging Research, University of Innsbruck, 6020 Innsbruck, Austria
[2]Division of Translational Cell Genetics, Medical University of Innsbruck, 6020 Innsbruck, Austria
[3]Department of Medical Epidemiology and Biostatistics, Karolinska Institute, 17177 Stockholm, Sweden
[4]Faculty of Medicine and Life Sciences, University of Tampere, Tampere 33014, Finland
[5]Department of Orthopedic Surgery, Hospital Wels-Grieskirchen, 4600 Wels, Austria
[6]These authors contributed equally
[7]Lead Contact
*Correspondence: andreas.meryk@uibk.ac.at
https://doi.org/10.1016/j.celrep.2019.02.024

SUMMARY

Fc receptor for IgM (FcμR)-deficient mice display dysregulated function of neutrophils, dendritic cells, and B cells. The relevance of FcμR to human T cells is still unknown. We show that FcμR is mostly stored inside the cell and that surface expression is tightly regulated. Decreased surface expression on T cells from elderly individuals is associated with alterations in the methylation pattern of the *FCMR* gene. Binding and internalization of IgM stimulate transport of FcμR to the cell surface to ensure sustained IgM uptake. Concurrently, IgM accumulates within the cell, and the surface expression of other receptors increases, among them the T cell receptor (TCR) and costimulatory molecules. This leads to enhanced TCR signaling, proliferation, and cytokine release, in response to low, but not high, doses of antigen. Our findings indicate that FcμR is an important regulator of T cell function and reveal an additional mode of interaction between B and T cells.

INTRODUCTION

The Fc receptor for IgM (FcμR) is a transmembrane protein initially referred to as "Fas apoptosis inhibitory molecule 3" (FAIM3) and TOSO (Hitoshi et al., 1998). IgM is bound with high avidity in a 1:1 stoichiometry of FcμR to IgM (Kubagawa et al., 2009; Shima et al., 2010; Vire et al., 2011). This feature of the receptor led to the misleading assumption of a potent inhibition of Fas/CD95-induced apoptosis in early studies (Hitoshi et al., 1998; Nguyen et al., 2011), which has now been disproved (Honjo et al., 2012b; Kubagawa et al., 2009). We recently demonstrated in FcμR-deficient mice that dysregulated function of neutrophils increased susceptibility to bacterial infection (Lang et al., 2013). Defects in the maturation and differentiation of dendritic cells also impaired viral control (Lang et al., 2015). Regarding adaptive immune cells, mice lacking the FcμR had increased IgG autoantibodies and natural IgM (Honjo et al., 2012a; Ouchida et al., 2012), enhanced differentiation of B-1 cells, and dysregulated homeostasis of B-2 cells (Nguyen et al., 2017a). Increased surface expression of IgM-BCR in FcμR-deficient B cells was demonstrated, and it was concluded that FcμR downregulates surface expression of IgM-BCR (Nguyen et al., 2017a). All mice studies have been performed without analyzing the consequence of IgM binding to its cognate receptor. In contrast to the situation in mice, human FcμR expression is restricted to B and T lymphocytes and, to a lesser extent, natural killer (NK) cells, but is not expressed by other hematopoietic cells (Kubagawa et al., 2009; Murakami et al., 2012). Human FcμR is overexpressed in B cell lymphomas (Vire et al., 2011) and has been linked to disease progression (Li et al., 2011; Pallasch et al., 2008). A functional characterization of FcμR in T cells is still missing, presumably because FcμR is absent on murine T cells (Nguyen et al., 2017a; Shima et al., 2010).

T cell activation is a crucial checkpoint in adaptive immunity. Signaling downstream of the T cell receptor (TCR) following antigenic stimulation results in proliferation, differentiation, and effector cytokine release. Dysregulated TCR activation may support immunodeficiency or autoimmunity (Notarangelo, 2014; Theofilopoulos et al., 2017). Cellular signaling is strictly regulated and is known to exhibit thresholds (Das et al., 2009; van den Berg et al., 2013). The number of triggered TCRs is essential, and a reduction of surface TCR expression severely compromises the capacity to reach the activation threshold (Viola and Lanzavecchia, 1996). With age, an increased TCR activation threshold leads to a reduced signaling capacity of the ERK pathway which impairs signal strength and activation of individual T cells (Li et al., 2012). In addition, extracellular factors such as the dose of antigen and the duration and the strength of TCR signaling influence T cell activation (Constant et al., 1995; Huppa et al., 2003; Kalergis et al., 2001; van Panhuys et al., 2014). We designed a study to investigate the consequences of IgM binding to FcμR on human T cells. We demonstrate that with T cell

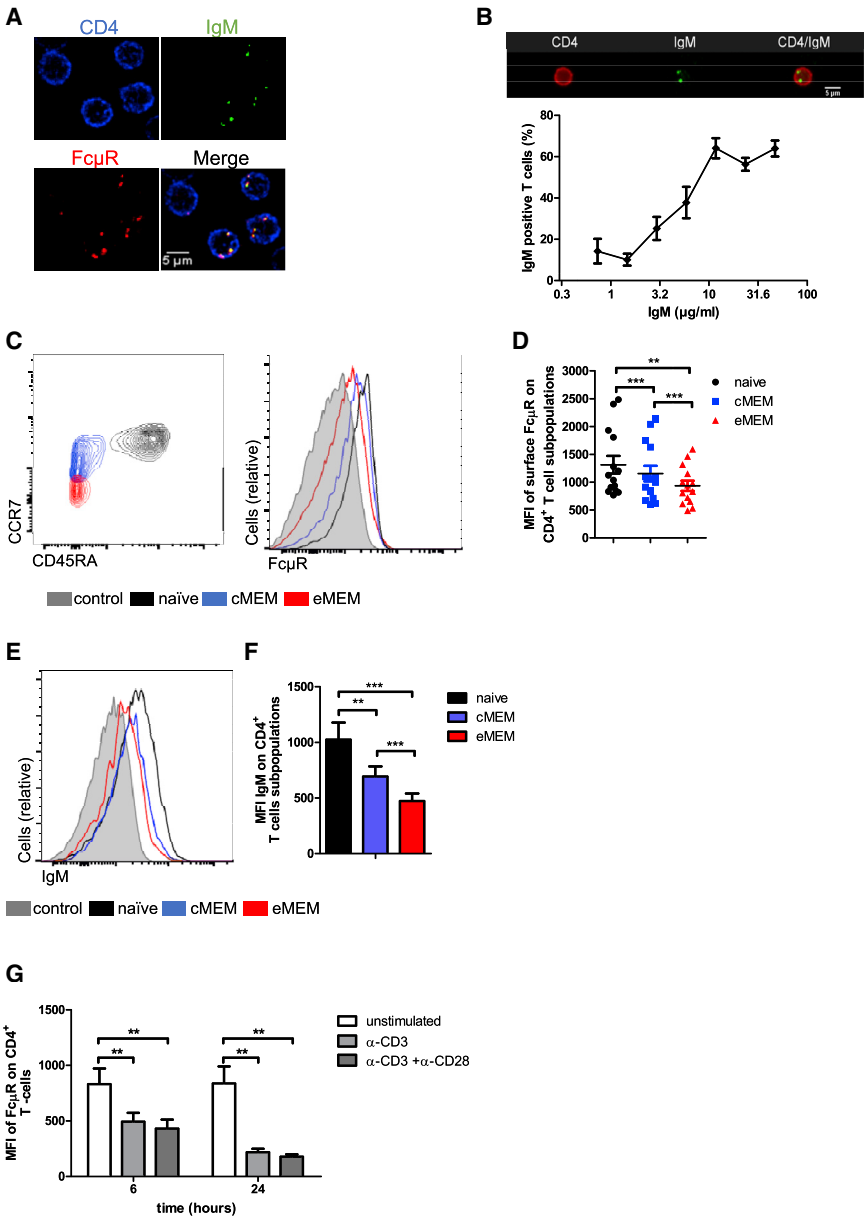

Figure 1. FcμR Enables Human T Cells to Bind IgM but Is Downregulated by Differentiation and TCR-Mediated Activation

(A) Confocal microscopy of CD4$^+$ T cells (blue), incubated with rabbit α-FcμR and IgM-Alexa 488 (green) for 2 h at 37°C in serum-free medium. Fixed and permeabilized cells were co-stained with secondary Cy3 α-rabbit (red) to visualize internalized FcμR.

(B) PBMCs were incubated for 2 h with IgM-Alexa 488 using concentrations between 0.7 and 47 μg/mL. IgM binding and internalization were quantified using ImageStream.

(C) Flow cytometry of PBMCs gated on live CD3$^+$CD4$^+$ T cells. A contour plot of naive (CCR7$^+$CD45RA$^+$, black), cMEM (CCR7$^+$CD45RA$^-$, blue), and eMEM (CCR7$^-$CD45RA$^-$, red) CD4$^+$ T cells is shown (left). Right: overlay histogram showing surface expression of FcμR protein on naive (black), cMEM (blue), and eMEM (red) CD4$^+$ T cells. Gray represents fluorescence minus one (FMO).

(D) Flow cytometry quantification of surface FcμR expression on CD4$^+$ T cells (gated as in C) and presented as change in mean fluorescence intensity (MFI).

(E and F) Flow cytometry analysis of IgM binding on naive, cMEM, and eMEM CD4$^+$ T cells and presented as change in MFI (F). Overlay histogram (E) showing IgM binding on naive (black), cMEM (blue), and eMEM (red) CD4$^+$ T cells. FMO control (without IgM-Alexa 488 incubation) is shown in gray.

(G) Magnetic-activated cell sorting (MACS) sorted CD4$^+$ T cells MACS were stimulated for 6 and 24 h with 1 μg/mL α-CD3 or 1 μg/mL α-CD3 plus 1 μg/mL α-CD28 in serum-free medium. Surface expression of FcμR on CD4$^+$ T cells was assessed using flow cytometry and presented as change in MFI.

Samples of six to ten donors per group pooled from at least three independent experiments (B–G) or one representative picture of three stained samples (A). Data are shown as mean ± SEM. $^{**}p < 0.01$ and $^{***}p < 0.001$ (Wilcoxon matched-pairs test). See also Figure S1.

differentiation, and following antigenic stimulation of the TCR, surface FcμR is strongly downregulated. FcμR expression is significantly reduced in naive and memory T cell populations from elderly people. Most FcμR is stored within the cell and traffics continuously to the cell membrane. Sustained FcμR expression on the cell surface leads to accumulation of the complex IgM:FcμR within the cell. Enrichment of IgM accelerates protein transport between the cell surface and the cell interior and thereby increases the expression of TCR and costimulatory molecules. Thus, FcμR-mediated binding of IgM increases TCR signaling, proliferation, and cytokine secretion of peripheral T cells. In contrast, bone marrow (BM) microenvironment downregulates surface FcμR expression, keeping the T cells in a resting state.

RESULTS

Differentiation and Activation of Human CD4$^+$ T Cells Downregulate Surface FcμR Expression

As demonstrated for B cells (Kubagawa et al., 2009; Nguyen et al., 2017a; Vire et al., 2011), IgM was also bound by the FcμR on CD4$^+$ T cells, and the complex FcμR:IgM was internalized (Figure 1A). ImageStream analysis demonstrated a concentration-dependent binding and internalization of IgM, reaching a peak between 10 and 50 μg/mL of IgM (Figure 1B). Next we analyzed FcμR expression on naive, central memory (cMEM), and effector memory (eMEM) CD4$^+$ T cells defined by the markers CCR7 and CD45RA (Figure 1C). With differentiation from naive to antigen-experienced T cells, FcμR expression decreased significantly

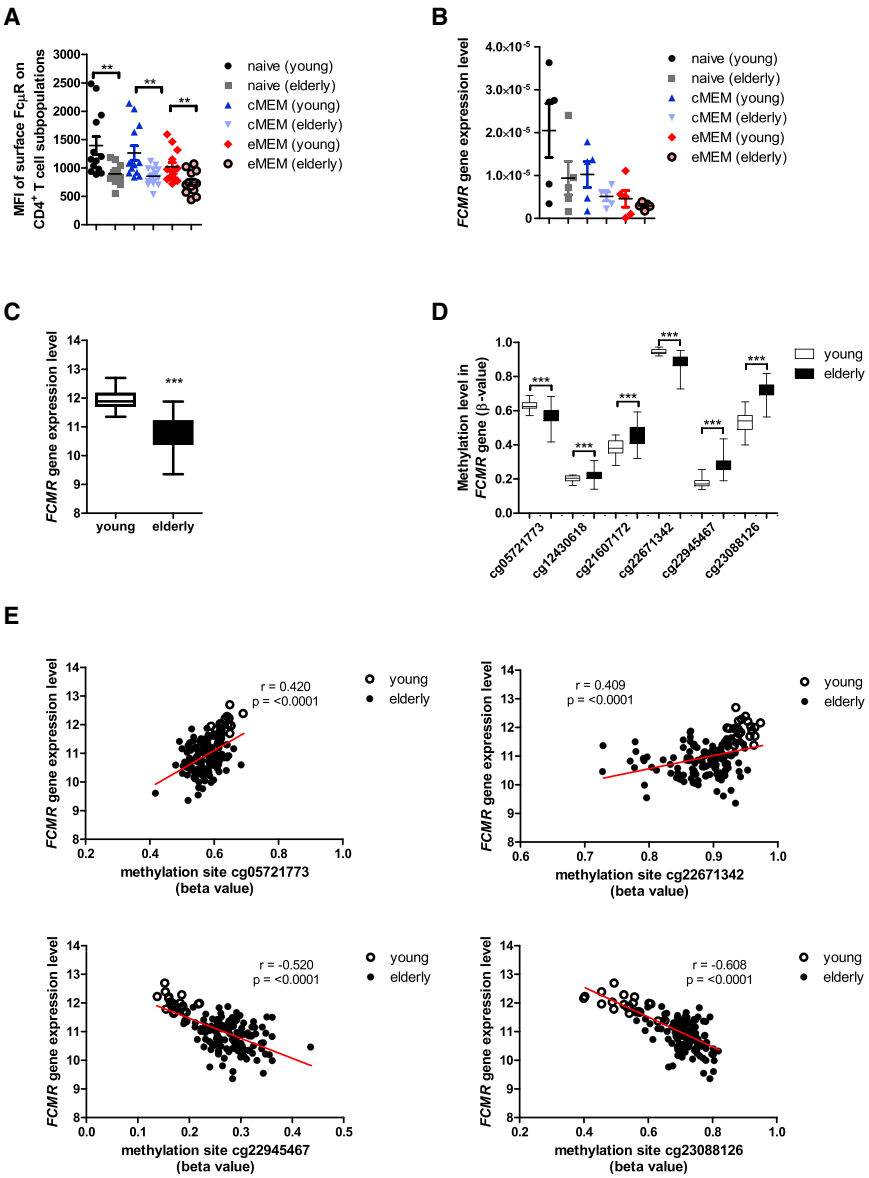

Figure 2. Reduced FcμR Expression on CD4+ T Cells Is Associated with Changes in *FCMR* Methylation during Aging

(A and B) PBMCs were obtained from young (<35 years) and elderly (>65 years) donors.

(A) Flow cytometry quantification of surface FcμR expression on naive, cMEM, and eMEM CD4+ T cells, presented as change in MFI.

(B) Naive, cMEM, and eMEM CD4+ T subpopulations were sorted using flow cytometry. Expression of *FCMR* mRNA, normalized to the control gene *β-Actin*, was measured.

(C–E) *FCMR* transcript and methylation pattern of the *FCMR* gene were analyzed in PBMC samples obtained from the Vitality 90+ study.

(C) Expression of *FCMR* mRNA and (D) age-related differences in methylation sites in *FCMR* gene from young and elderly donors.

(E) Correlations of the methylation sites cg05721773, cg22671342, cg22945467, and cg23088126 with *FCMR* mRNA.

Five to 13 samples per group pooled from at least three independent experiments (A and B). Twenty-one young and 122 old individuals derived from the Vitality 90+ study (C–E). Data are shown as mean ± SEM. *p < 0.05, **p < 0.01, and ***p < 0.001 (unpaired Mann-Whitney test, A–D). Each dot point represents one individual. Spearman's coefficient (r) and p value are shown in the graph (E). See also Figure S2 and Table S1.

these data demonstrate that FcμR is highly expressed on the surface of naive PB CD4+ T cells, which enables them to bind high amounts of IgM. Following TCR-mediated activation and with differentiation, FcμR expression declines on T cells.

Age-Related Alterations in the Methylation of the *FCMR* Gene Decrease mRNA and Protein Expression

Aging leads to a progressive diminution of the naive and expansion of the eMEM T cell compartment (Grubeck-Loebenstein et al., 1998; Linton and Dorshkind, 2004). To assess whether this change was reflected by low FcμR expression, we analyzed the expression of FcμR on the subpopulations of CD4+ T cells from healthy young (<35 years) and elderly (>65 years) persons. FcμR expression was decreased on naive and memory CD4+ T cells obtained from elderly donors compared with their counterparts from young donors (Figure 2A). Consistently, IgM binding was strongly reduced on all CD4+ T cell subpopulations from elderly individuals (Figure S2). Because naive and antigen-experienced T cells were equally affected, the expansion of memory T cells was presumably not the only cause of decreased FcμR protein in CD4+ T cells from elderly persons. We were therefore interested in whether transcriptional and genomic regulatory mechanisms were involved. For this purpose, we purified CD4+ T cell

on peripheral blood (PB) CD4+ T cells (Figure 1D). Consequently, naive CD4+ T cells bound significantly more IgM than cMEM and eMEM T cells, as indicated by their higher mean fluorescence intensity of IgM (Figures 1E and 1F). The CD8+ T cell compartment also showed a downregulation of surface FcμR expression from naive to antigen-experienced cells (Figure S1A), but the surface FcμR was lower on naive and cMEM CD8+ T cells compared with their CD4+ T cell counterparts (Figure S1A). In line with the surface expression, CD8+ T cells bound and internalized lower amounts of IgM compared with CD4+ T cells (Figure S1B). A hallmark of T cells is their capacity to expand and differentiate after TCR-mediated activation. Thus, we investigated whether signaling via the TCR could influence FcμR expression. Six and 24 h after αCD3 or αCD3 plus αCD28-mediated TCR activation, FcμR protein was strongly downregulated (Figure 1G). Together

subpopulations from young and elderly persons. Consistent with surface protein expression, the *FCMR* mRNA expression level was highest in naive CD4 T cells obtained from young donors (Figure 2B). The mRNA transcript decreased with age and differentiation. To strengthen our observation that aging leads to decreased mRNA transcript, we analyzed *FCMR* mRNA and its association with the methylation levels in the *FCMR* gene in more than 100 PB mononuclear cell (PBMC) samples obtained from the Vitality 90+ study (Marttila et al., 2015). The expression of *FCMR* transcripts was significantly downregulated in elderly individuals (Figure 2C). Next we examined whether the 16 methylation sites in the *FCMR* gene that were present in the Illumina 450k array were affected by age. Six of these sites showed differential methylation between young and elderly individuals (Figure 2D). A significant correlation between *FCMR* transcript and methylation level was observed for 4 of these sites (Figure 2E; Table S1). DNA methylation is known to regulate gene expression, but the exact mechanisms are unknown. Promoter methylation, however, typically represses gene expression by blocking the binding of transcription factors. One of the 4 sites, cg22945467, is located upstream of a transcription start site (TSS1500); hence, the observed inverse correlation between the methylation level on this site and *FCMR* expression aligns with the scenario of hypermethylation leading to downregulated expression. This findings suggest that the aging-associated alterations in *FCMR* methylation could affect its expression in an age-dependent manner. Age-related alterations of surface receptors may at least partially contribute to decreased T cell response in old age (Li et al., 2012), but a potential impact of FcμR on T cell function has not yet been investigated.

Tissue Microenvironment Modulates Surface FcμR Expression Independent from an Intracellular Reservoir

Confocal microscopy of the T cell zone from human tonsil indicated FcμR localization on the cell surface as well as inside the cell (Figure 3A). Thus, we examined FcμR in permeabilized and non-permeabilized PB CD4$^+$ T cells. A strong intracellular presence of FcμR compared with the surface was visible (Figure 3B). For a better quantification, surface and intracellular expression was measured using flow cytometry. Just a small proportion of the total FcμR protein was detected on the cell surface (Figure 3C). Again, surface FcμR decreased with differentiation from naive to antigen-experienced cells, whereas the highest intracellular protein amount was present in cMEM T cells (Figure 3D). After antigen clearance, antigen-specific T cells migrate to the BM, where they reside as long-lived memory cells (Pangrazzi et al., 2017; Tokoyoda et al., 2009). To check whether this affects either surface or intracellular FcμR expression, we isolated CD4$^+$ T cells from BM and PB of the same donor. In every donor, the expression of FcμR was significantly lower on BM CD4$^+$ T cells compared with the corresponding PB CD4$^+$ T cell subpopulations (Figures 3E, 3F, and S3A). BM CD4$^+$ T cells still stored large amounts of FcμR within the cell but significantly less compared with PB CD4$^+$ T cell subpopulations (Figures 3E and 3F). We speculated whether the BM environment might affect the surface expression of FcμR. Indeed, 20 h culture in serum-free medium raised the surface expression of FcμR on BM CD4$^+$ T cells (Figure 3G). Typical BM T cell survival cytokines might be responsible for decreased FcμR surface expression. Therefore, we treated BMMCs for 20 h with IL-6, IL-7, and IL-15 or combinations of these cytokines. With the exception of IL-6 alone, these cytokines downregulated the surface expression of FcμR on BMMCs (Figure 3H) and even more on PB CD4$^+$ T cells (Figure S3B) during 20 h culture. Our data indicate a tissue-specific regulation of surface FcμR expression mediated by the microenvironment. The FcμR is stored within T cells. Presumably, fast re-expression on the surface is therefore possible when BM T cells migrate from the BM back to the blood.

Intracellular FcμR Traffics Continuously to the Cell Surface Leading to IgM Enrichment Inside the Cell

We wondered why T cells store large amounts of FcμR. Thus we investigated the possibility of whether intracellular FcμR traffics continuously to the plasma membrane and back. To address this point, T cells were incubated with α-FcμR antibody (Ab) at 4°C for 30 min, washed, and shifted to 37°C for 20 h. During this second incubation step, FcμR disappeared from the cell surface but could still be found in the cytoplasm (Figure 4A, top). In contrast, strong intracellular and surface FcμR staining was visible when cells were incubated in the presence of α-FcμR Ab at 37°C for 20 h (Figure 4A, bottom). To provide further evidence of possible FcμR recycling between the cell interior and the plasma membrane, we treated CD4$^+$ T cells with actinomycin D, brefeldin A, MG132, and IgM for 20 h in the presence of α-FcμR Ab. As expected, membrane trafficking was totally inhibited by brefeldin A but was not influenced by actinomycin D and MG132, suggesting that neither *de novo* synthesis nor proteasomal degradation of FcμR played a major role (Figure 4B). Surprisingly, even in the presence of IgM, an increased amount of FcμR was expressed on the cell surface (Figure 4B), indicating that even following IgM-mediated internalization, receptor recycling took place. To investigate the functional impact of FcμR recycling, we incubated CD4$^+$ T cells with IgM and α-FcμR Ab for 2 and 20 h and documented IgM uptake by confocal microscopy. IgM internalization increased, and IgM and FcμR were highly enriched within the cells after 20 h compared with 2 h (Figure 4C). Flow cytometry confirmed the observed IgM enrichment during 20 h culture (Figure 4D). To study whether endocytosis might be involved in IgM uptake, we stained early endosomes. After 2 h, internalized IgM co-localized with EEA1 (early) endosomes (Figure 4E). As control for specific co-localization of IgM and EEA1 and to exclude coincidental overlay, we stained for Rab7 (late) and Rab11 (recycling). Both endosomal markers did not co-localize with IgM. These data show that FcμR traffics continuously to the plasma membrane, aiming to catch as much IgM as possible. The internalized IgM accumulates within the cell rather than being degraded.

FcμR Acts as a Costimulatory Molecule Enhancing TCR Signaling, Proliferation, and Cytokine Production

The function of FcμR and the consequences of IgM internalization and enrichment in T cells have not yet been investigated. Because IgM accumulates in T cells over time, we analyzed T cell proliferation, administrating IgM prior to and

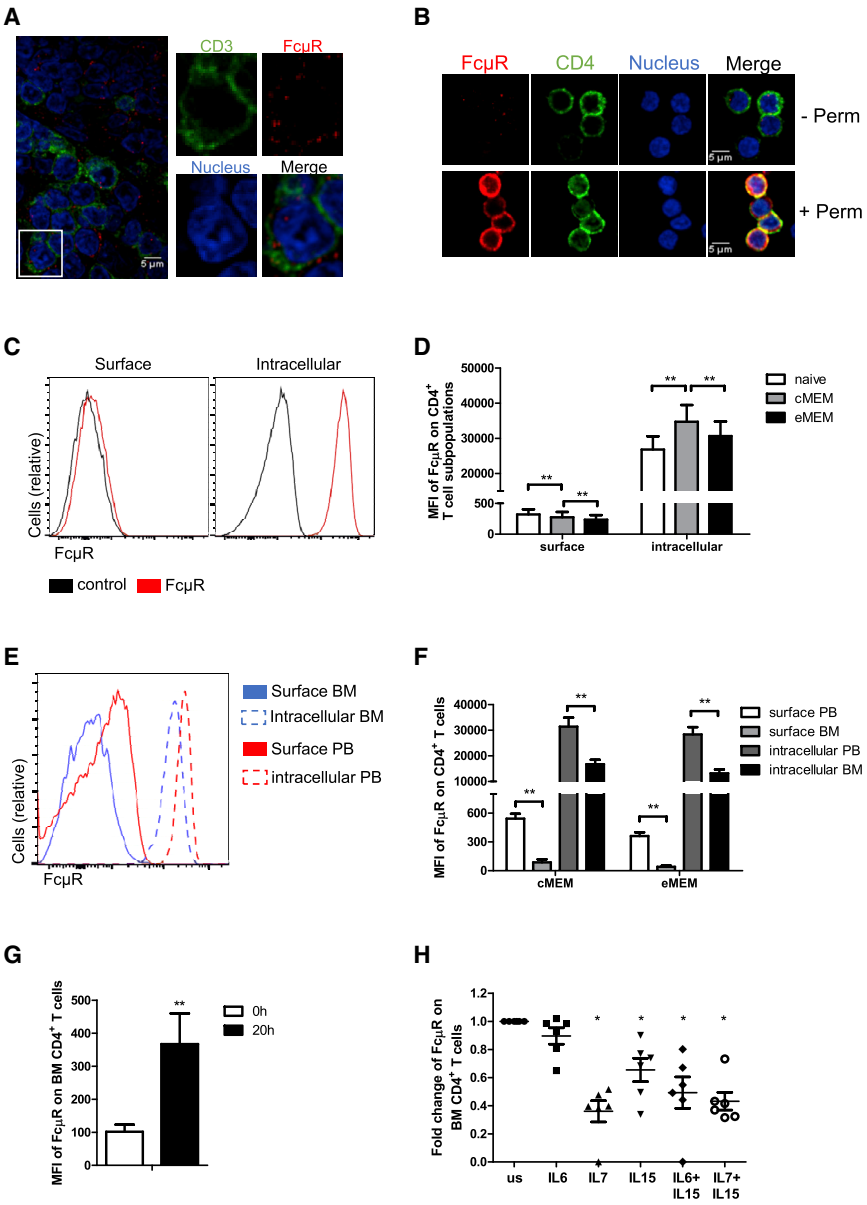

Figure 3. Tissue-Specific Regulation of Surface and Intracellular FcμR Expression

(A) Confocal microscopy of a paraffin-embedded tonsil stained with α-CD3 (green), DAPI (blue), and α-FcμR (red).

(B) Confocal microscopy of non-permeabilized (-perm; top) and permeabilized (+perm; bottom) $CD4^+$ T cells, stained with α-CD4 (green), DAPI (blue), and α-FcμR (red).

(C and D) Flow cytometry analysis of surface and intracellular expression of FcμR protein on naive, cMEM, and eMEM $CD4^+$ T cells (D). Overlay histogram (C) showing surface (left) and intracellular (right) expression of FcμR protein (red) and control staining (FMO; black).

(E and F) Surface and intracellular expression of FcμR protein on cMEM and eMEM T cells from PB and BM of the same donor (F). Overlay histogram (E) showing surface and intracellular expression of FcμR protein on cMEM $CD4^+$ T cells. PB surface (red, solid), BM surface (blue, solid), PB intracellular (red, dashed), and BM intracellular (blue, dashed) are shown.

(G) Surface expression of FcμR on BM $CD4^+$ T cells was measured directly after isolation of BM mononuclear cells (BMMCs) (0 h) and after 20 h culture at 37°C in serum-free medium.

(H) BMMCs were incubated for 20 h with 100 ng/mL of IL-6, IL-7, IL-15, or a combination of 100 ng/mL IL-6 and IL-15 or IL-7 and IL-15 in serum-free medium. Surface expression of FcμR on BM $CD4^+$ T cells was measured using flow cytometry, and the fold change of untreated samples was calculated.

Eight to ten samples per group pooled from at least three independent experiments (C–H) or one representative picture of three stained samples and tissues (A and B). Data are shown as mean ± SEM. *$p < 0.05$ and **$p < 0.01$ (Wilcoxon matched-pairs test). See also Figure S3.

simultaneously with TCR-mediated activation. Twenty hours of preincubation with IgM significantly enhanced $CD4^+$ and $CD8^+$ T cell proliferation (Figures 5A, 5B, and S4A). This effect was absent following simultaneous administration of IgM and TCR stimuli (Figures 5A and 5B) or following preincubation with IgM for a period shorter than 20 h (Figure S4B). In contrast, two recent studies showed an inhibitory effect of IgM on T cell proliferation but did not provide an explanation for the underlying mechanism (Colucci et al., 2015; Lloyd et al., 2017). Experiments in both studies were performed in RPMI-1640 supplemented with 10% fetal bovine serum (FBS) using high concentrations of TCR stimuli (α-CD3/α-CD28-coated beads or PMA) and IgM purchased from Sigma. Sigma IgM contains sodium azide, whereas Jackson IgM (purchased from Jackson Immunoresearch), used in our experiments, is free of any preservative. We therefore analyzed whether this might explain the discrepancy between the results (Figures S4C and S4D). Adding sodium azide to Jackson IgM results in reduced proliferation (Figures S4E and S4F), whereas the dialyzation of Sigma IgM diminished the inhibitory effect (Figure S4G). Using the standard T cell culture medium RPMI plus 10% fetal calf serum (FCS), we could not observe any difference in T cell proliferation in response to additional IgM (Figure S4H). FCS contains large amounts of natural IgM, and we cannot exclude that the human FcμR interacts with calf IgM. Therefore, we performed our experiments in serum-free medium optimized for T cell culture.

To provide further evidence of a costimulatory function of FcμR, we stimulated PBMCs with different concentrations of αCD3 plus αCD28. IgM increased T cell proliferation when TCR stimuli were limited, and a high concentration of αCD3 plus αCD28 (10 μg/mL) overrode the need for FcμR-mediated costimulation (Figure 5C). To determine whether IgM binding to FcμR on $CD4^+$ T cells is responsible for increased proliferation

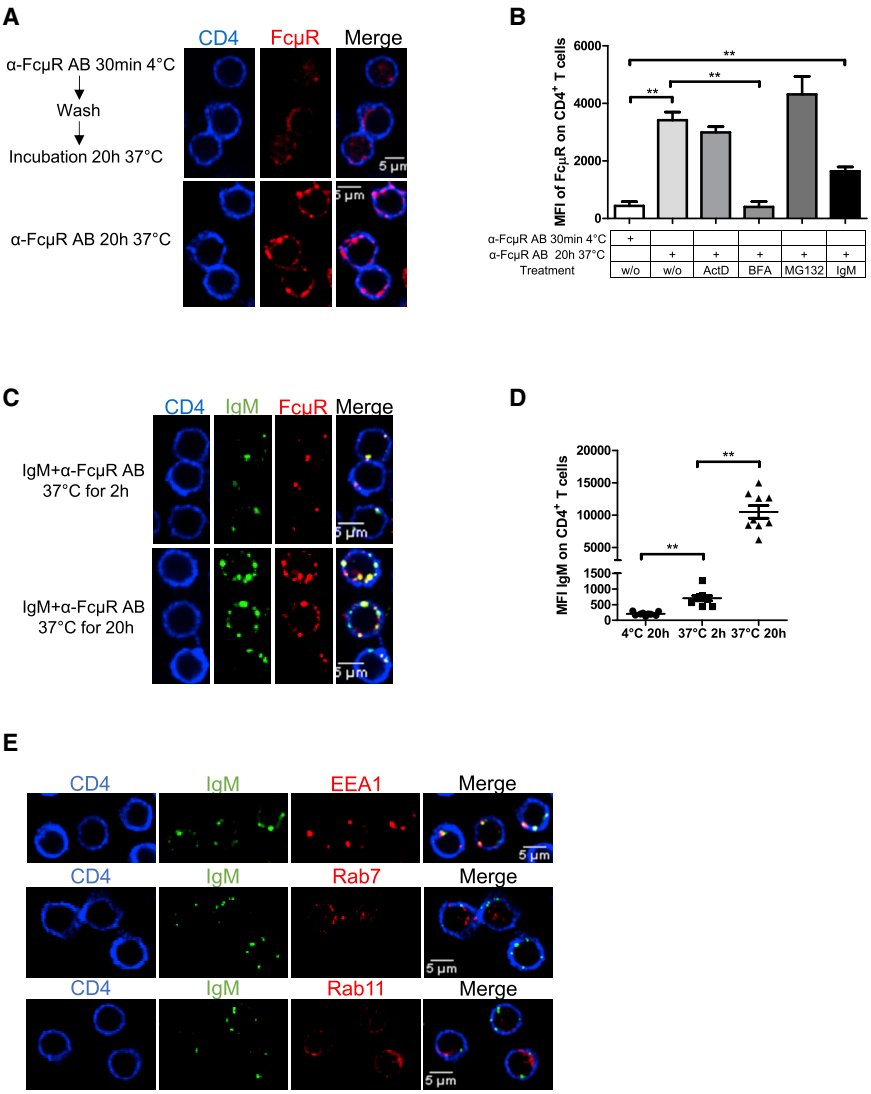

Figure 4. FcμR Trafficking between Cell Surface and Cell Interior Results in IgM Enrichment

(A) PBMCs were incubated for 30 min at 4°C with rabbit α-FcμR Ab, then washed and shifted to 37°C for 20 h (top) in serum-free medium. Bottom: cells were incubated for 20 h at 37°C in the presence of α-FcμR Ab in serum-free medium. After surface staining with α-CD4 (blue), cells were fixed, permeabilized, and stained with secondary α-rabbit Cy3 (red).

(B) PBMCs were incubated either for 30 min at 4°C with rabbit α-FcμR Ab or for 20 h at 37°C in the presence of α-FcμR Ab in serum-free medium. In addition, cells were pretreated for 0.5 h with 10 μg/mL brefeldin A (BFA), 20 ng/mL actinomycin D (ActD), or 1 μM MG132 prior to α-FcμR Ab incubation. Alternatively, 47 μg/ml IgM was added together with α-FcμR Ab. After surface staining of $CD3^+CD4^+$ T cells, cells were fixed, permeabilized, and stained with secondary α-rabbit Alexa 647.

(C) Confocal microscopy of T cells, incubated for 2 and 20 h at 37°C with rabbit α-FcμR AB and 47 μg/ml IgM-Alexa 488 (green) in serum-free medium. After washing, cells were stained with α-CD4 (blue) and then fixed and permeabilized. Cells were co-stained with secondary α-rabbit Cy3 (red) to visualize surface and internalized FcμR.

(D) PBMCs were incubated for 2 h at 37°C or 20 h at 4°C and 37°C with 47 μg/mL IgM-Alexa 488. Flow cytometry analysis of IgM binding on $CD4^+$ T cells presented as change in MFI.

(E) PBMCs were incubated for 2 h at 37°C with 47 μg/mL IgM-Alexa 488 (green). After surface staining with α-CD4 (blue), cells were fixed, permeabilized, and stained with α-EEA1 (top), α-Rab7 (middle), or α-Rab11 (bottom) plus secondary anti-rabbit-Cy3 (red).

Eight or nine samples per group pooled from at least three independent experiments (B and D) or one representative picture of three stained samples and tissues (A, C, and E). Data are shown as mean ± SEM. **$p < 0.01$ (Wilcoxon matched-pairs test).

or whether this effect is mediated by other cells, we purified $CD4^+$ T cells from PB. $CD4^+$ T cells stimulated with αCD3, or αCD3 plus αCD28 proliferated faster, and the frequency of $CD25^+$ cells was strongly increased by IgM preincubation (Figures 5D–5F). Next, we were interested in whether the continuous presence of IgM influences T cell activation after several stimulation cycles, or whether it induces exhaustion. First PBMCs were stimulated with αCD3, then with IL-2, and finally with different combinations of αCD3 and IL-2 (Figure S5A). $CD4^+$ T cells continuously stimulated in the presence of IgM kept proliferation increased 3 and 4 days after the last activation cycle (Figures S5B and S5C). Next, we quantified the production of IFNγ over a time period of 48 h. IgM preincubation led to an increased IFNγ secretion of $CD4^+$ T cells stimulated with αCD3 or αCD3 plus αCD28 at all time points (Figure 5G).

To understand how IgM acts on the distal effector functions of TCR and CD28 signaling, including proliferation and cytokine production, we investigated signaling events following TCR and CD28 engagement. We preincubated purified $CD4^+$ T cells with IgM for 20 h or left them untreated before TCR stimulation. Phosphorylation of ERK1/2 was altered by IgM preincubation and strongly enhanced after 30 min of activation with αCD3 plus αCD28 (Figures 5H and S5D). In contrast activation of the classical NFκB pathway was not altered, as measured by phosphorylation of IκBα (Figures 5H and S5E). Along this line, proximal TCR signaling investigated by analysis of Zap-70 (Tyr319) phosphorylation was not significantly altered 1, 3, or 5 min after activation of IgM-treated or untreated cells (data not shown). Costimulatory function of FcμR after activation therefore does not influence early proximal TCR signaling but converges later, specifically at the Erk1/2 signaling pathway. Our findings show that preincubation with IgM boosts TCR signaling, proliferation, and cytokine production when antigen exposure is relatively low.

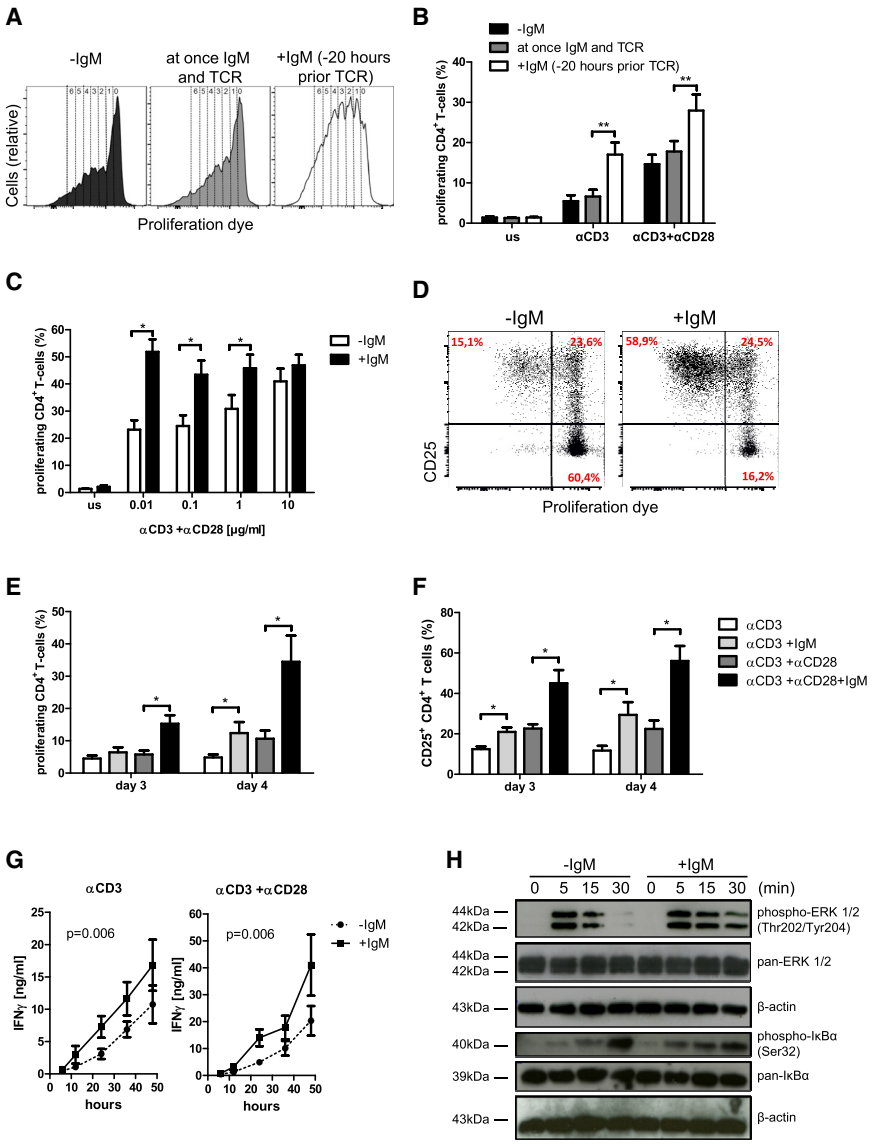

Figure 5. Intracellular Accumulation of IgM Enhances T Cell Proliferation, Cytokine Production, and Signaling

(A and B) IgM (47 μg/mL) was administered to division tracking-labeled PBMCs, 20 h prior to or simultaneously with TCR stimulation using 1 μg/mL α-CD3 or 1 μg/mL α-CD3 plus 1 μg/mL α-CD28 in serum-free medium. As control, PBMCs were kept in serum-free medium without IgM.

(A) Representative histograms of $CD4^+$ T cells without IgM treatment (left), simultaneous IgM treatment and TCR engagement (middle), or pre-incubated with IgM (right).

(B) Proliferation of $CD4^+$ T cells with or without IgM administration was measured using flow cytometry at day 4 after stimulation.

(C) IgM (47 μg/mL) was administered to division tracking-labeled PBMCs, 20 h prior to stimulation (+IgM). As control, PBMCs were kept in serum-free medium without IgM (−IgM). PBMCs were stimulated with the indicated concentrations of α-CD3 plus α-CD28 in serum-free medium. Proliferation of $CD4^+$ T cells was quantified using flow cytometry at day 4 after stimulation.

(D–F) MACS-sorted $CD4^+$ T cells were pre-incubated for 20 h with 47 μg/mL IgM (+IgM) or kept in serum-free medium (−IgM). After pre-incubation, T cells were transferred to plates coated with 1 μg/mL α-CD3, and 1 μg/mL soluble α-CD28 was added to some wells.

(D) Dot plots show CD25 expression and proliferation of control (−IgM, left) and IgM-pre-incubated (+IgM, right) $CD4^+$ T cells following activation with α-CD3 plus α-CD28 at day 4. Red numbers indicate the frequency of cells in each quadrant.

(E and F) Proliferation (E) and expression of CD25 (F) were quantified using flow cytometry at days 3 and 4 after stimulation.

(G) MACS-sorted $CD4^+$ T cells were preincubated for 20 h with 47 μg/mL IgM (+IgM) or kept in serum-free medium (−IgM). Supernatants were collected after 6, 12, 24, and 48 h after transfer to plates coated with 1 μg/mL α-CD3, and 1 μg/mL soluble α-CD28 was added to some wells. ELISAs for IFNγ of α-CD3 (left) or α-CD3 plus α-CD28 (right) activated cells were performed.

(H) MACS-sorted $CD4^+$ T cells were preincubated for 20 h with 47 μg/mL IgM (+IgM) or kept in serum-free medium (−IgM). After preincubation, T cells were transferred to plates coated with 1 μg/mL α-CD3, and 1 μg/mL soluble α-CD28 was added. Cells were harvested at indicated time points. Immunoblotting analysis of total and phosphorylated ERK1/2 and IκBα was performed.

Six to 19 samples per group pooled from at least three independent experiments (A–G) or one representative gel out of three (H). Data are shown as mean ± SEM. *$p < 0.05$ and **$p < 0.01$ (Wilcoxon matched-pairs test in B, C, E, and F or two-way ANOVA in G). See also Figures S4 and S5.

Intracellular Accumulation of IgM Increases Surface Expression of TCR and CD28 by Regulating Protein Transport to the Cell Surface

We demonstrated that T cells ensured high IgM uptake, which then led to increased TCR signaling. Because of the increased phosphorylation of ERK1/2, we focused on upstream molecules of the TCR pathway, which might be modulated by IgM enrichment. IgM preincubation enhanced surface expression of CD3 and CD28 on $CD4^+$ T cells (Figures 6A and 6B). Consistent with the FcμR expression profile on $CD4^+$ and $CD8^+$ T cell subpopulations (Figures 1D and S1A), the percentage increase of CD3 and CD28 was higher on naive $CD4^+$ and $CD8^+$ T cells compared with antigen-experienced T cells (Figures 6C and S6A–S6C). The increased surface expression of the molecules induced by IgM was not due to alterations in gene transcription (Figure 6D). Generally, TCR expression is dependent on a balance of *de novo* synthesis, recycling, and degradation (Geisler, 2004). To investigate which of these pathways were most affected, we incubated PBMCs with IgM in the presence of actinomycin D, cycloheximide, or MG132. TCR expression was strongly enhanced by IgM regardless of inhibition of mRNA transcription, protein synthesis, or proteasomal

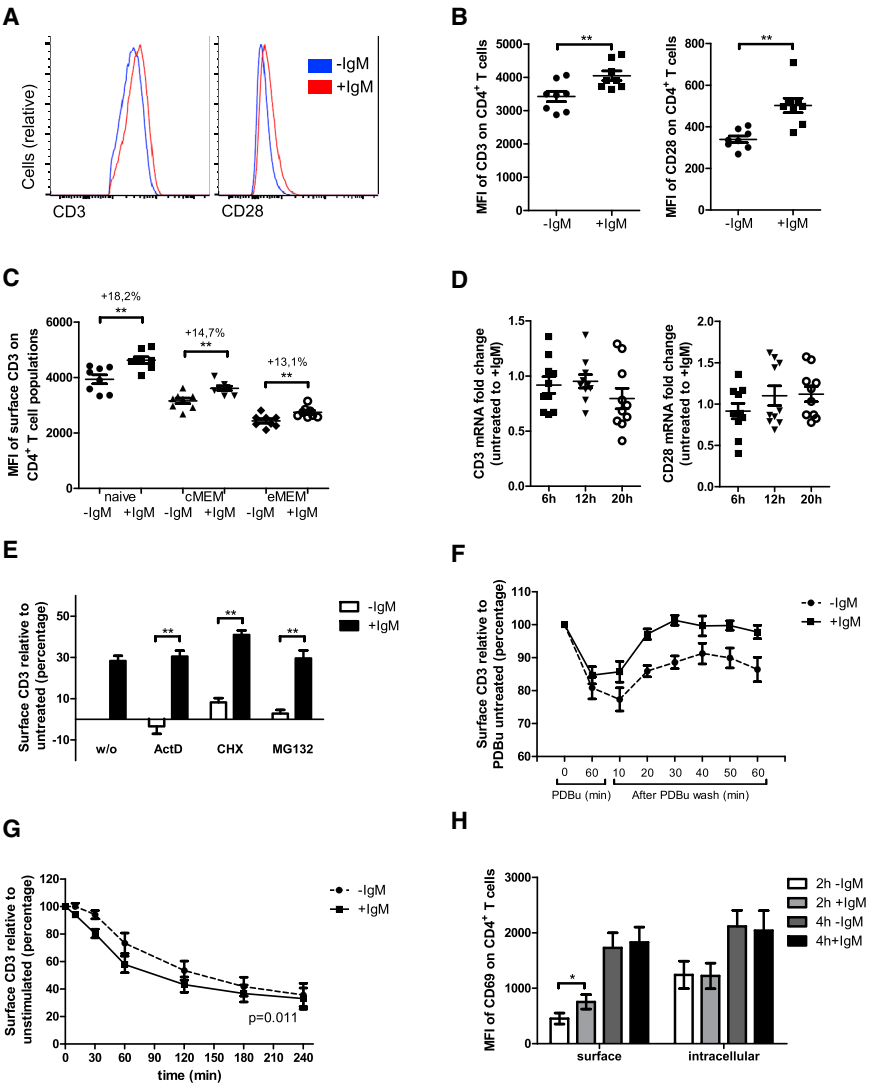

Figure 6. IgM Accumulation within CD4⁺ T Cells Accelerates Protein Transport

(A–C) PBMCs were incubated for 20 h with 47 μg/mL IgM (+IgM) or kept in serum-free medium (−IgM). Expression of CD3 and CD28 was measured using flow cytometry.

(A) Overlay histograms showing surface expression of CD3 (left) and CD28 (right) on −IgM (blue) and +IgM (red) CD4⁺ T cells.

(B) MFI of CD3 (left) and CD28 (right) on CD4⁺ T cells.

(C) MFI of CD3 was quantified on naive, cMEM, and eMEM CD4⁺ T cells. Numbers indicate the percentage increase as average of all samples, calculated as change in percentage (% = MFI of CD3 on IgM preincubated cells/MFI of CD3 on control cells × 100).

(D) MACS-sorted CD4⁺ T cells were incubated for 6, 12, and 20 h with 47 μg/mL IgM or kept in serum-free medium, and the expression of *CD3* (left) and *CD28* (right) mRNA, normalized to the control gene *β-Actin*, was measured. Fold changes between IgM preincubated and control cells are shown.

(E) PBMCs were incubated for 20 h with 10 μg/mL cycloheximide, 20 ng/mL actinomycin D, or 1 μM MG132 or kept untreated in serum-free medium in the presence (+IgM) or absence (−IgM) of 47 μg/mL IgM. Expression of CD3 was quantified using flow cytometry. Percentage change in surface CD3 expression normalized to control cells without IgM administration is shown.

(F) Relative levels of CD3 in IgM preincubated (+IgM) and control (−IgM) cells, which were untreated or treated with PDBu for 1 h. After PDBu treatment, cells were washed and incubated at 37°C for the indicated times. Percentage change in surface CD3 expression normalized to untreated cells.

(G) PBMCs were incubated for 20 h with 47 μg/mL IgM (+IgM) or kept in serum-free medium (−IgM). After 20 h, cells were activated with mouse α-CD3 at 37°C for the indicated times and then shifted to ice and stained with α-mouse fluorescein isothiocyanate (FITC). Percentage change in surface CD3 expression normalized to unstimulated cells (0 min).

(H) PBMCs were preincubated with 47 μg/mL IgM (+IgM) or left untreated (−IgM), then cells were stimulated for 2 and 4 h using 1 μg/mL α-CD3 plus 1 μg/mL α-CD28 in the presence or absence of 10 μg/mL BFA in serum-free medium. After washing, CD4⁺ T cells were stained for surface and intracellular CD69 expression. MFI of CD69 was calculated as change in MFI (ΔMFI = MFI of stimulated cells − MFI of non-stimulated cells).

Six to ten samples per group pooled from at least three independent experiments (A–H). Data are shown as mean ± SEM. *$p < 0.05$ and **$p < 0.01$ (Wilcoxon matched pairs test in (B–F and H or two-way ANOVA in G). See also Figure S6.

degradation (Figure 6E). Therefore, we focused on TCR recycling between the cytoplasmic pool and the cell surface, assuming that protein transport might play a role. Control and IgM-preincubated cells were treated with PDBu (phorbol 12,13-dibutyrate) for 1 h, which resulted in ~20% TCR internalization (Figure 6F). The time course of surface CD3 recovery after PDBu removal was monitored using flow cytometry. IgM-preincubated cells recovered surface CD3 within 30 min, while control cells did not reach basal level in the observation time (Figure 6F). Next, PBMCs were incubated with IgM for 20 h or left untreated, and internalization of CD3 following TCR engagement was measured using flow cytometry. Preincubation with IgM enhanced internalization of CD3 (Figure 6G).

To evaluate whether FcμR acts specifically on TCR recycling or generally on protein transport, we measured the kinetics of the *de novo* synthesized protein CD69 on the cell surface and within the cell. Two hours following TCR activation, the amount of intracellular CD69 was similar in IgM-preincubated and control cells, but surface expression was significantly increased (Figure 6H). Consistent with a general effect of FcμR on protein transport, the expression of CCR7 and CD45RA was also increased by IgM preincubation (Figures S6D and S6E). These data suggest that FcμR controls and regulates the speed of protein transport between the cell interior and the cell surface and therefore also the surface expression of the TCR and of costimulatory molecules.

DISCUSSION

It is well understood that IgM Ab is a first line of host defense. We propose that B cells support T cell activation by the secretion of IgM, which then binds to the FcμR on T lymphocytes. Entering the splenic white pulp, naive T cells have to pass through the marginal zone (MZ). In humans, the splenic MZ contains memory B cells with a high surface density of IgM, which are activated rapidly and secrete IgM in response to antigenic challenge (Cerutti et al., 2013). To our knowledge, the IgM concentrations in the interstitial spaces of tissues such as spleen and lymph node (LN) have never been determined. We suggest that naive T cells entering the spleen and LN receive an IgM boost, resulting in enhanced surface expression of TCR and costimulatory molecules (Figures 6B and 6C). T cell activation occurs when a threshold of approximately 8,000 TCRs (Viola and Lanzavecchia, 1996) or at least 30%–50% of TCRs (Valitutti et al., 1996) are triggered. Thus, IgM uptake mediated by the FcμR on naive T cells would facilitate to reach the activation threshold, in particular when inflammatory conditions and antigen concentrations are low. High antigen concentrations make FcμR-mediated stimulation unnecessary (Figure 5C). A similar observation was described in $Fc\mu R^{flx/flx}$ CD19-cre mice infected with the influenza virus (Nguyen et al., 2017b). In mixed BM chimeras, FcμR-deficient B cells had a significant competitive disadvantage in their ability to differentiate into plasma cells. Interestingly, reduced plasma cell frequencies were not observed when mice received a high-dose influenza virus infection. Therefore, the authors concluded an intrinsic requirement for FcμR expression on B cells for plasma cell differentiation, but only when influenza virus doses were low. In line with our postulated function of IgM on T cells, selective IgM deficiency in humans is associated with increased morbidity and mortality from various bacterial, viral, and fungal infections (Louis and Gupta, 2014). In patients with IgM deficiency, severe decreases in the number and function of $CD4^+$ T cell have been documented (De la Concha et al., 1982; Gharib et al., 2015). Also with aging, the severity and the incidence of infections increase, accompanied by diminished function of T cells in elderly people (Grubeck-Loebenstein et al., 1998; Li et al., 2012). We observed that genomic regulation of the *FCMR* gene by DNA methylation is associated with reduced expression of the transcript and protein (Figures 2A, 2C, and 2E) and therefore could, at least partially, contribute to reduced T cell function in elderly individuals.

The long-term survival of memory T cells in the BM is mediated by cytokine- and chemokine-producing stromal and myeloid cells forming specific areas known as BM niches. Memory $CD4^+$ T cells are attracted mainly to $IL7^+$-producing cells, whereas memory $CD8^+$ T cells are in close vicinity to IL-15-producing cells, a cytokine that in synergy with IL-6 supports homeostatic proliferation and survival of $CD8^+$ T cells (Herndler-Brandstetter et al., 2011; Pangrazzi et al., 2017; Tokoyoda et al., 2009). BM memory T cells preserve a quiescent state but can be reactivated quickly and efficiently. This is in accordance with our data showing that the FcμR stimulates T cell activation and function, but that low surface expression of FcμR on BM memory $CD4^+$ T cells seems to prevent this. Consistent with the notion that $CD4^+$ memory T cell survival depends mainly on IL-7 producing cells, we observed the strongest *in vitro* downregulation of surface FcμR expression on $CD4^+$ T cells by this cytokine (Figures 3H and S3B). Because most of the FcμR protein is stored within the cell (Figure 3F), BM T cells were capable of rapidly increasing their FcμR surface expression in the absence of the BM microenvironment *in vitro* (Figure 3G). In doing this, BM T cells could ensure a fast re-expression of FcμR on the surface when they migrate from the BM back to the blood *in vivo*.

A similar distribution is described for CTLA-4, which is localized primarily in intracellular compartments and whose surface expression is tightly regulated by restricted trafficking to the cell surface. CTLA-4 is found mainly in the *trans* Golgi network, in endosomes and secretory vesicles (Leung et al., 1995). Translocation of CTLA-4 to the cell surface occurs at the immunological synapse and is regulated by the strength of TCR signaling (Darlington et al., 2002). In contrast to CTLA-4, the FcμR traffics to the surface of resting cells (Figures 4A and 4B), and TCR engagement downregulates this process. In resting T cells, FcμR binds and internalizes IgM, which leads to additional transport of the receptor to the cell surface to ensure sustained IgM uptake (Figure 4B). In accordance with this idea, our data show that IgM accumulates within the cell over time (Figure 4D). Short-term exposure to IgM was not sufficient in achieving T cell activation *in vitro* (Figures 5B and S4B). The duration of IgM exposure may therefore be an important determinant for the activation threshold. Under physiological conditions, T cells have a retention time in lymphatic organs of 12 to 24 h before they egress back to the blood (Cyster, 2005). This period is even longer at the onset of an immune response (Benechet et al., 2016). IgM effects on T cells during this time may be a perquisite for T cell activation.

When internalized IgM accumulates within the cell, the surface expression of the TCR and the costimulatory molecule CD28 is upregulated (Figures 6B and 6C). Enhanced surface TCR expression was independent of RNA or protein synthesis (Figures 6D and 6E), but may be due to changes within the cytoskeleton. Molecules involved in actin as well as microtubule-associated protein transport are involved in regulation of TCR surface expression (Finetti et al., 2009; Hao et al., 2013). Further studies will be necessary to identify the intracellular binding partner of IgM and/or IgM:FcμR which triggers accelerated protein transport.

In light of the fact that FcμR deficiency in mice influences activation of very diverse signaling events in granulocytes, monocytes, dendritic cells, and B cells (Brenner et al., 2014; Lang et al., 2013, 2015; Nguyen et al., 2017a), we assume that FcμR influences a variety of different molecules possibly via the same mechanism. Our data indicate that protein transport in both directions, from the cell surface into the cell and vice versa, is accelerated by IgM (Figures 6F and 6G). Stimulation of protein transport to the cell surface was not restricted to the TCR and costimulatory molecules, but IgM preincubation also increased the surface expression of other receptors, such as CD69 and CD45RA (Figures 6H and S6E). A recent publication on $Fc\mu r^{flx/flx}CD19^+$cre mice demonstrated that FcμR decelerates the surface transport of the IgM-BCR but not IgD-BCR. FcμR-deficient B cells had increased BCR expression, which resulted in enhanced tonic BCR signaling (Nguyen

et al., 2017a). In concept with our data, FcμR-deficient immature dendritic cells showed reduced surface expression of CD80, CD86, and major histocompatibility complex (MHC) II, even after stimulation with various Toll-like receptor ligands (Brenner et al., 2014). The functional impact of IgM binding to FcμR was not addressed in these studies. Additionally, only in B cells, would FcμR be capable of binding to IgM-BCR within the cell, and therefore hinder surface expression.

In summary, we report that FcμR promotes protein transport to the cell surface of human T cells and thus enhances cell signaling, proliferation, and cytokine secretion. We also demonstrate that binding of IgM by the FcμR increases the expression of TCR-unrelated surface molecules when intracellular IgM enrichment takes place. This highlights the importance of B cell and T cell interactions in the early stages of an immune response. IgM may be a useful tool in increasing T cell activation when required but may, on the other hand, be deleterious by enhancing autoreactivity in the case of autoimmune diseases.

STAR★METHODS

Detailed methods are provided in the online version of this paper and include the following:

- KEY RESOURCES TABLE
- CONTACT FOR REAGENT AND RESOURCE SHARING
- EXPERIMENTAL MODEL AND SUBJECT DETAILS
  - Human subjects
- METHOD DETAILS
  - Cell culture and T cell activation
  - Isolation of RNA and quantitative RT-PCR
  - Flow cytometry
  - Cell Sorting
  - ImageStream
  - Immunofluorescence analysis of tonsil biopsies
  - Immunofluorescence confocal microscopy
  - ELISA assay
  - Western blot
- QUANTIFICATION AND STATISTICAL ANALYSIS

SUPPLEMENTAL INFORMATION

Supplemental Information can be found with this article online at https://doi.org/10.1016/j.celrep.2019.02.024.

ACKNOWLEDGMENTS

We are grateful to Alexandar Tzankov (University Hospital Basel) for providing tonsil biopsies, to Sieghart Sopper and Petra Schumacher (Medical University Innsbruck) for flow cytometry sorting of $CD4^+$ T cell subpopulations, and to Erin Naismith (University of Innsbruck) for critical reading of the manuscript. This work was supported by the European Union (EU) H2020 project "An Integrated Approach to Dissect Determinants, Risk Factors, and Pathways of Ageing of the Immune System" (ImmunoAgeing, H2020-PHC-2014 grant agreement 633964). The research leading to these results also received funding from the EU's Seventh Framework Programme (FP7/2007-2013) under grant agreement 280873, "Advanced Immunization Technologies" (ADITEC), and the FWF Austrian Science Fund (P28694-B30). L.P. was supported by a DOC fellowship funded by the Austrian Academy of Sciences. The funders had no role in study design, data collection and analysis, decision to publish, or preparation of the manuscript.

AUTHOR CONTRIBUTIONS

A.M. designed, performed, and supervised experiments, analyzed data, and wrote the manuscript. G.B. provided help with experimental design. L.P., M.H., F.H., B. Jakic, and N.H.-K. performed experiments and analyzed data. B. Jenewein helped with confocal microscopy. J.J. performed the analyses of DNA methylation and gene expression in the Vitality 90+ sample. M.H. provided the facilities for the array-based gene expression and DNA methylation analyses in the Vitality 90+ sample. K.T. provided paired BM and PB samples and helped with experimental design. B.G.-L. designed and supervised experiments and provided support in writing the manuscript. All authors provided edits to the manuscript.

DECLARATION OF INTERESTS

The authors declare no competing interests.

Received: August 30, 2018
Revised: January 28, 2019
Accepted: February 7, 2019
Published: March 5, 2019

REFERENCES

Benechet, A.P., Menon, M., Xu, D., Samji, T., Maher, L., Murooka, T.T., Mempel, T.R., Sheridan, B.S., Lemoine, F.M., and Khanna, K.M. (2016). T cell-intrinsic S1PR1 regulates endogenous effector T-cell egress dynamics from lymph nodes during infection. Proc. Natl. Acad. Sci. U S A *113*, 2182–2187.

Brenner, D., Brüstle, A., Lin, G.H., Lang, P.A., Duncan, G.S., Knobbe-Thomsen, C.B., St Paul, M., Reardon, C., Tusche, M.W., Snow, B., et al. (2014). Toso controls encephalitogenic immune responses by dendritic cells and regulatory T cells. Proc. Natl. Acad. Sci. U S A *111*, 1060–1065.

Cerutti, A., Cols, M., and Puga, I. (2013). Marginal zone B cells: virtues of innate-like antibody-producing lymphocytes. Nat. Rev. Immunol. *13*, 118–132.

Colucci, M., Stöckmann, H., Butera, A., Masotti, A., Baldassarre, A., Giorda, E., Petrini, S., Rudd, P.M., Sitia, R., Emma, F., and Vivarelli, M. (2015). Sialylation of N-linked glycans influences the immunomodulatory effects of IgM on T cells. J. Immunol. *194*, 151–157.

Constant, S., Pfeiffer, C., Woodard, A., Pasqualini, T., and Bottomly, K. (1995). Extent of T cell receptor ligation can determine the functional differentiation of naive CD4+ T cells. J. Exp. Med. *182*, 1591–1596.

Cyster, J.G. (2005). Chemokines, sphingosine-1-phosphate, and cell migration in secondary lymphoid organs. Annu. Rev. Immunol. *23*, 127–159.

Darlington, P.J., Baroja, M.L., Chau, T.A., Siu, E., Ling, V., Carreno, B.M., and Madrenas, J. (2002). Surface cytotoxic T lymphocyte-associated antigen 4 partitions within lipid rafts and relocates to the immunological synapse under conditions of inhibition of T cell activation. J. Exp. Med. *195*, 1337–1347.

Das, J., Ho, M., Zikherman, J., Govern, C., Yang, M., Weiss, A., Chakraborty, A.K., and Roose, J.P. (2009). Digital signaling and hysteresis characterize ras activation in lymphoid cells. Cell *136*, 337–351.

De la Concha, E.G., Garcia-Rodriguez, M.C., Zabay, J.M., Laso, M.T., Alonso, F., Bootello, A., and Fontan, G. (1982). Functional assessment of T and B lymphocytes in patients with selective IgM deficiency. Clin. Exp. Immunol. *49*, 670–676.

Finetti, F., Paccani, S.R., Riparbelli, M.G., Giacomello, E., Perinetti, G., Pazour, G.J., Rosenbaum, J.L., and Baldari, C.T. (2009). Intraflagellar transport is required for polarized recycling of the TCR/CD3 complex to the immune synapse. Nat. Cell Biol. *11*, 1332–1339.

Geisler, C. (2004). TCR trafficking in resting and stimulated T cells. Crit. Rev. Immunol. *24*, 67–86.

Gharib, A., Louis, A.G., Agrawal, S., and Gupta, S. (2015). Syndrome of selective IgM deficiency with severe T cell deficiency associated with disseminated cutaneous mycobacterium avium intracellulaire infection. Am. J. Clin. Exp. Immunol. *4*, 15–27.

Grubeck-Loebenstein, B., Berger, P., Saurwein-Teissl, M., Zisterer, K., and Wick, G. (1998). No immunity for the elderly. Nat. Med. *4*, 870.

Hao, Y.H., Doyle, J.M., Ramanathan, S., Gomez, T.S., Jia, D., Xu, M., Chen, Z.J., Billadeau, D.D., Rosen, M.K., and Potts, P.R. (2013). Regulation of WASH-dependent actin polymerization and protein trafficking by ubiquitination. Cell *152*, 1051–1064.

Herndler-Brandstetter, D., Landgraf, K., Jenewein, B., Tzankov, A., Brunauer, R., Brunner, S., Parson, W., Kloss, F., Gassner, R., Lepperdinger, G., and Grubeck-Loebenstein, B. (2011). Human bone marrow hosts polyfunctional memory CD4+ and CD8+ T cells with close contact to IL-15-producing cells. J. Immunol. *186*, 6965–6971.

Hitoshi, Y., Lorens, J., Kitada, S.I., Fisher, J., LaBarge, M., Ring, H.Z., Francke, U., Reed, J.C., Kinoshita, S., and Nolan, G.P. (1998). Toso, a cell surface, specific regulator of Fas-induced apoptosis in T cells. Immunity *8*, 461–471.

Honjo, K., Kubagawa, Y., Jones, D.M., Dizon, B., Zhu, Z., Ohno, H., Izui, S., Kearney, J.F., and Kubagawa, H. (2012a). Altered Ig levels and antibody responses in mice deficient for the Fc receptor for IgM (FcμR). Proc. Natl. Acad. Sci. U S A *109*, 15882–15887.

Honjo, K., Kubagawa, Y., and Kubagawa, H. (2012b). Is Toso an antiapoptotic protein or an Fc receptor for IgM? Blood *119*, 1789–1790.

Huppa, J.B., Gleimer, M., Sumen, C., and Davis, M.M. (2003). Continuous T cell receptor signaling required for synapse maintenance and full effector potential. Nat. Immunol. *4*, 749–755.

Kalergis, A.M., Boucheron, N., Doucey, M.A., Palmieri, E., Goyarts, E.C., Vegh, Z., Luescher, I.F., and Nathenson, S.G. (2001). Efficient T cell activation requires an optimal dwell-time of interaction between the TCR and the pMHC complex. Nat. Immunol. *2*, 229–234.

Kubagawa, H., Oka, S., Kubagawa, Y., Torii, I., Takayama, E., Kang, D.W., Gartland, G.L., Bertoli, L.F., Mori, H., Takatsu, H., et al. (2009). Identity of the elusive IgM Fc receptor (FcmuR) in humans. J. Exp. Med. *206*, 2779–2793.

Lang, K.S., Lang, P.A., Meryk, A., Pandyra, A.A., Boucher, L.M., Pozdeev, V.I., Tusche, M.W., Göthert, J.R., Haight, J., Wakeham, A., et al. (2013). Involvement of Toso in activation of monocytes, macrophages, and granulocytes. Proc. Natl. Acad. Sci. U S A *110*, 2593–2598.

Lang, P.A., Meryk, A., Pandyra, A.A., Brenner, D., Brüstle, A., Xu, H.C., Merches, K., Lang, F., Khairnar, V., Sharma, P., et al. (2015). Toso regulates differentiation and activation of inflammatory dendritic cells during persistence-prone virus infection. Cell Death Differ. *22*, 164–173.

Leung, H.T., Bradshaw, J., Cleaveland, J.S., and Linsley, P.S. (1995). Cytotoxic T lymphocyte-associated molecule-4, a high-avidity receptor for CD80 and CD86, contains an intracellular localization motif in its cytoplasmic tail. J. Biol. Chem. *270*, 25107–25114.

Li, F.J., Kubagawa, Y., McCollum, M.K., Wilson, L., Motohashi, T., Bertoli, L.F., Barton, J.C., Barnes, S., Davis, R.S., and Kubagawa, H. (2011). Enhanced levels of both the membrane-bound and soluble forms of IgM Fc receptor (FcμR) in patients with chronic lymphocytic leukemia. Blood *118*, 4902–4909.

Li, G., Yu, M., Lee, W.W., Tsang, M., Krishnan, E., Weyand, C.M., and Goronzy, J.J. (2012). Decline in miR-181a expression with age impairs T cell receptor sensitivity by increasing DUSP6 activity. Nat. Med. *18*, 1518–1524.

Linton, P.J., and Dorshkind, K. (2004). Age-related changes in lymphocyte development and function. Nat. Immunol. *5*, 133–139.

Lloyd, K.A., Wang, J., Urban, B.C., Czajkowsky, D.M., and Pleass, R.J. (2017). Glycan-independent binding and internalization of human IgM to FCMR, its cognate cellular receptor. Sci. Rep. *7*, 42989.

Louis, A.G., and Gupta, S. (2014). Primary selective IgM deficiency: an ignored immunodeficiency. Clin. Rev. Allergy Immunol. *46*, 104–111.

Marttila, S., Kananen, L., Häyrynen, S., Jylhävä, J., Nevalainen, T., Hervonen, A., Jylhä, M., Nykter, M., and Hurme, M. (2015). Ageing-associated changes in the human DNA methylome: genomic locations and effects on gene expression. BMC Genomics *16*, 179.

Murakami, Y., Narayanan, S., Su, S., Childs, R., Krzewski, K., Borrego, F., Weck, J., and Coligan, J.E. (2012). Toso, a functional IgM receptor, is regulated by IL-2 in T and NK cells. J. Immunol. *189*, 587–597.

Nguyen, X.H., Lang, P.A., Lang, K.S., Adam, D., Fattakhova, G., Föger, N., Kamal, M.A., Prilla, P., Mathieu, S., Wagner, C., et al. (2011). Toso regulates the balance between apoptotic and nonapoptotic death receptor signaling by facilitating RIP1 ubiquitination. Blood *118*, 598–608.

Nguyen, T.T., Kläsener, K., Zürn, C., Castillo, P.A., Brust-Mascher, I., Imai, D.M., Bevins, C.L., Reardon, C., Reth, M., and Baumgarth, N. (2017a). The IgM receptor FcμR limits tonic BCR signaling by regulating expression of the IgM BCR. Nat. Immunol. *18*, 321–333.

Nguyen, T.T.T., Graf, B.A., Randall, T.D., and Baumgarth, N. (2017b). sIgM-FcμR interactions regulate early B cell activation and plasma cell development after influenza virus infection. J. Immunol. *199*, 1635–1646.

Notarangelo, L.D. (2014). Immunodeficiency and immune dysregulation associated with proximal defects of T cell receptor signaling. Curr. Opin. Immunol. *31*, 97–101.

Ouchida, R., Mori, H., Hase, K., Takatsu, H., Kurosaki, T., Tokuhisa, T., Ohno, H., and Wang, J.Y. (2012). Critical role of the IgM Fc receptor in IgM homeostasis, B-cell survival, and humoral immune responses. Proc. Natl. Acad. Sci. U S A *109*, E2699–E2706.

Pallasch, C.P., Schulz, A., Kutsch, N., Schwamb, J., Hagist, S., Kashkar, H., Ultsch, A., Wickenhauser, C., Hallek, M., and Wendtner, C.M. (2008). Overexpression of TOSO in CLL is triggered by B-cell receptor signaling and associated with progressive disease. Blood *112*, 4213–4219.

Pangrazzi, L., Meryk, A., Naismith, E., Koziel, R., Lair, J., Krismer, M., Trieb, K., and Grubeck-Loebenstein, B. (2017). "Inflamm-aging" influences immune cell survival factors in human bone marrow. Eur. J. Immunol. *47*, 481–492.

Schindelin, J., Arganda-Carreras, I., Frise, E., Kaynig, V., Longair, M., Pietzsch, T., Preibisch, S., Rueden, C., Saalfeld, S., Schmid, B., et al. (2012). Fiji: an open-source platform for biological-image analysis. Nat. Methods *9*, 676–682.

Shima, H., Takatsu, H., Fukuda, S., Ohmae, M., Hase, K., Kubagawa, H., Wang, J.Y., and Ohno, H. (2010). Identification of TOSO/FAIM3 as an Fc receptor for IgM. Int. Immunol. *22*, 149–156.

Theofilopoulos, A.N., Kono, D.H., and Baccala, R. (2017). The multiple pathways to autoimmunity. Nat. Immunol. *18*, 716–724.

Tokoyoda, K., Zehentmeier, S., Hegazy, A.N., Albrecht, I., Grün, J.R., Löhning, M., and Radbruch, A. (2009). Professional memory CD4+ T lymphocytes preferentially reside and rest in the bone marrow. Immunity *30*, 721–730.

Valitutti, S., Müller, S., Dessing, M., and Lanzavecchia, A. (1996). Different responses are elicited in cytotoxic T lymphocytes by different levels of T cell receptor occupancy. J. Exp. Med. *183*, 1917–1921.

van den Berg, H.A., Ladell, K., Miners, K., Laugel, B., Llewellyn-Lacey, S., Clement, M., Cole, D.K., Gostick, E., Wooldridge, L., Sewell, A.K., et al. (2013). Cellular-level versus receptor-level response threshold hierarchies in T-cell activation. Front. Immunol. *4*, 250.

van Panhuys, N., Klauschen, F., and Germain, R.N. (2014). T-cell-receptor-dependent signal intensity dominantly controls CD4(+) T cell polarization in vivo. Immunity *41*, 63–74.

Viola, A., and Lanzavecchia, A. (1996). T cell activation determined by T cell receptor number and tunable thresholds. Science *273*, 104–106.

Vire, B., David, A., and Wiestner, A. (2011). TOSO, the Fcmicro receptor, is highly expressed on chronic lymphocytic leukemia B cells, internalizes upon IgM binding, shuttles to the lysosome, and is downregulated in response to TLR activation. J. Immunol. *187*, 4040–4050.

STAR★METHODS

KEY RESOURCES TABLE

REAGENT or RESOURCE	SOURCE	IDENTIFIER
Antibodies		
Anti-CD3 (VioGreen) clone REA613	Miltenyi Biotec	Cat#130-109-545; RRID:AB_2657066
Anti-CD3 (FITC) clone REA613	Miltenyi Biotec	Cat#130-113-700; RRID:AB_2726241
Anti-CD3 (PeVio770) clone REA613	Miltenyi Biotec	Cat#130-113-140; RRID:AB_2725968
Anti-CD3 (APCVio770) clone REA613	Miltenyi Biotec	Cat#130-113-136; RRID:AB_2725964
Anti-CD3 (APC) clone SK7	BD Bioscience	Cat#345767
Anti-CD3 (purified, LEAF) clone OKT3	Biolegend	Cat#317304; RRID:AB_571925
Anti-CD4 (VioGreen) clone REA623	Miltenyi Biotec	Cat#130-109-456; RRID:AB_2657981
Anti-CD4 (BV421) SK3	BD Bioscience	Cat#565997; RRID:AB_2739448
Anti-CD4 (BV510) clone SK3	BD Bioscience	Cat#562970; RRID:AB_2744424
Anti-CD4 (Pe) clone SK3	BD Bioscience	Cat#565999; RRID:AB_2739450
Anti-CD4 (APC) clone RPA-T4	BD Bioscience	Cat#555349; RRID:AB_398593
Anti-CD8 (VioBlue) clone REA734	Miltenyi Biotec	Cat#130-110-683; RRID:AB_2659239
Anti-CD8 (PeVio770) clone REA734	Miltenyi Biotec	Cat#130-110-680; RRID:AB_2659245
Anti-CD8 (APC) clone RPA-T8	BD Bioscience	Cat#555369; RRID:AB_398595
Anti-CD8 (PerCP-Cy5.5) clone RPA-T8	BD Bioscience	Cat#565310; RRID:AB_2687497
Anti-CD25 (Pe) clone 2A3	BD Bioscience	Cat#341011
Anti-CD28 (purified, LEAF) clone CD28.2	Biolegend	Cat#302914; RRID:AB_314316
Anti-CD28 (Pe) clone L293	BD Bioscience	Cat#348047; RRID:AB_400368
Anti-CD28 (PeVio770) clone REA 612	Miltenyi Biotec	Cat#130-109-443; RRID:AB_2656958
Anti-CD45 (BV500) clone HI30	BD Bioscience	Cat#560777; RRID:AB_1937324
Anti-CD45RA (PE) clone REA562	Miltenyi Biotec	Cat#130-108-714; RRID:AB_2658307
Anti-CD69 (PE) clone FN50	BD Bioscience	Cat#555531; RRID:AB_395916
Anti-CCR7 (BV421) clone 150503	BD Bioscience	Cat#562555; RRID:AB_2728119
Anti-CCR7 (FITC) clone 150503	BD Bioscience	Cat#561271; RRID:AB_10561679
Rabbit anti-human FcμR	Sigma Aldrich	Cat#HPA003910; RRID:AB_1078798
Donkey anti-rabbit IgG (Alexa647) clone poly4064	Biolegend	Cat#406414; RRID:AB_2563202
Donkey anti-mouse IgG (Alexa488)	Abcam	Cat#ab150105; RRID:AB_2732856
Goat anti-rabbit (Cy3)	Abcam	Cat#ab97075; RRID:AB_10679955
7AAD	Miltenyi Biotec	Cat#130-111-568
Anti-β-actin	Santa Cruz Biotechnology	Cat#sc-1615; RRID:AB_630835
Anti-phospo-IκBα (Ser32) clone 14D4	Cell signaling	Cat#2859; RRID:AB_561111
Anti-IκBα	Cell signaling	Cat#9242; RRID:AB_331623
Anti-phospho-ERK1/2 (Thr202/Tyr204)	Cell signaling	Cat#9101; RRID:AB_331646
Anti-ERK1/2	Cell signaling	Cat#9102; RRID:AB_330744
Anti-EEA1 (C45B10)	Cell signaling	Cat#3288; RRID:AB_2096811
Anti-Rab7 (D95F2)	Cell signaling	Cat#9367; RRID:AB_1904103
Anti-Rab11 (D4F5)	Cell signaling	Cat#5589; RRID:AB_10693925
ChromPure Human IgM	Jackson ImmunoResearch	Cat#009-000-012; RRID:AB_2337048
ChromPure Human IgM (Alexa488).	Jackson ImmunoResearch	Cat#009-540-012; RRID:AB_2337105
IgM from human serum	Sigma Aldrich	Cat#I8260; RRID:AB_1163621
Chemicals, Peptides, and Recombinant Proteins		
Actinomycin D	Sigma Aldrich	Cat#A1410
BFA	Sigma Aldrich	Cat#B6542

(*Continued on next page*)

Continued

REAGENT or RESOURCE	SOURCE	IDENTIFIER
Collagenase (CLSPA)	Worthington Biochemical	Cat#LS005273
Cyclohexamide	Sigma Aldrich	Cat#01810
Dapi	Sigma Aldrich	Cat#D9542
Ficoll-Hypaque	VWR	Cat#17-1440-03
Fluorescent mounting medium	Dako	Cat#S3023
MG132	Sigma Aldrich	Cat#474787
Penicillin-Streptomycin	Sigma Aldrich	Cat#P0781
Phorbol 12,13-dibutyrate (PDBu)	Sigma Aldrich	Cat#P1269
Recombinant human IL-6 protein	Immunotools	Cat# 11340066
Recombinant human IL-7 protein	Immunotools	Cat# 11340073
Recombinant human IL-15 protein	Immunotools	Cat# 11340153
serum-free medium (TexMACS)	Miltenyi Biotec	Cat#130-097-196
Violet Proliferation Dye 450	BD Bioscience	Cat# 562158
Critical Commercial Assays		
Cytofix/Cytoperm kit	BD Bioscience	Cat#554714
CD4+ T Cell Isolation Kit	Miltenyi Biotec	Cat#130-096-533
IFNγ Elisa	Biolegend	Cat#430105
Reverse Transcription system	Promega	Cat#A3500
RNeasy Plus mini kit	QIAGEN	Cat#74134
SYBR Green	Roche Diagnostics	Cat#4887352001
TrueStain FcX	Biolegend	Cat#422302
Zombie Violet Fixable Viability Kit	Biolegend	Cat#423114
Pan T Cell Isolation Kit	human Miltenyi Biotec	Cat#130-096-535
Oligonucleotides		
β-actinFW 5′-TCTCCTTCTGCATTCTGTCG-3′	MWG Biotech	N/A
β-actinRW 5′-TCCTCCCTGGGCATGGAG-3′	MWG Biotech	N/A
CD3eFW 5′-GGGATCACCGCCTATGTT-3′	MWG Biotech	N/A
CD3eRW 5′-TCCTCCCTGGGCATGGAG-3′	MWG Biotech	N/A
CD28FW 5′- GAGAAGAGCAATGGAACCATTATC-3′	MWG Biotech	N/A
CD28RW 5′- TAGCAAGCCAGGACTCCACCAA-3′ FcmrFW 5’-TCACAGTCTGGGAGGGAA-3’ FcmrRW 5’-CATCCTCACGGCCAGTC-3′	MWG Biotech	N/A
Software and Algorithms		
Flowjo version 10.1	FlowJo LLC	N/A
GraphPad Prism version 5	GraphPad Software	N/A
IDEAS version 6.0340.0	Amnis	N/A
ImageJ version 1.48	NIH	N/A
Cell Voyager CV1000 version 1.06	Yokogawa	N/A
Primer3	http://simgene.com/Primer3	N/A

CONTACT FOR REAGENT AND RESOURCE SHARING

Further information and request for resources and reagents should be directed to and will be fulfilled by the Lead Contact, Andreas Meryk (andreas.meryk@uibk.ac.at).

EXPERIMENTAL MODEL AND SUBJECT DETAILS

Human subjects

Human BM and blood samples were obtained from systemically healthy individuals who did not receive immunomodulatory drugs or suffer from diseases known to influence the immune system, including autoimmune diseases and cancer. Hip replacement surgery

was performed and bone from the femur shaft was harvested. A biopsy of substantia spongiosa osseum, which would otherwise have been discarded, was used to isolate BM mononuclear cells (BMMCs). BM biopsies were fragmented, washed once with RPMI medium and treated with purified collagenase (CLSPA, Worthington Biochemical; 20U/mL) for 1hour at 37°C. BM biopsies were then centrifuged and BMMCs purified by density gradient centrifugation (Ficoll-Hypaque). Purification of PB mononuclear cells (PBMCs) from heparinized blood was also performed by density gradient centrifugation. $CD4^+$ T cells were isolated from PBMCs by negative selection with MACS (Miltenyi).

Most of the experiments were performed using samples obtained from human subjects younger than 35 years (in total 27 donors participated, aged from 21 to 34 years). For the comparison between young and elderly donors (> 65 years), samples from 13 participants aged between 67 and 84 years were obtained. The response to IgM were always investigated by comparing the cells obtained from the same donor (-/+ IgM). The experiments were conducted in a blinded fashion and were matched for age and sex, and groups contained 40%–60% of each sex. Sex-related differences were not observed.

The human subjects used in the array-based expression and DNA methylation analyses were derived from the Vitality 90+ study. These samples, the processing of the DNA methylation (Illumina 450k array) and expression data (Illumina HumanHT12v4 BeadChip) have been previously described in detail (Marttila et al., 2015). Study approval was given by Ethic Committee of Innsbruck Medical University (Austria) and the local institutions. Written informed consent was received from all participants prior to their inclusion in the study in accordance with the Declaration of Helsinki

METHOD DETAILS

Cell culture and T cell activation

PBMCs and purified $CD4^+$ T cells were cultivated in serum-free medium (TexMACS; Miltenyi) supplemented with 100 U/mL penicillin and 100 μg/mL streptomycin (Invitrogen). Cells were preincubated with ChromPure Human IgM (Jackson ImmunoResearch) or Alexa488 ChromPure Human IgM (Jackson ImmunoResearch). For proliferation, PBMCs and purified $CD4^+$ T cells were labeled with 1μM Violet Proliferation Dye (BD). 100.000 cells were activated with α-CD3 (Biolegend; clone OKT3) alone or plus α-CD28 (Biolegend; clone CD28.2). Both antibodies were added soluble to PBMCs but using purified $CD4^+$ T cells α-CD3 were coated to the plates in PBS overnight. Proliferation was determined by calculating the proliferation index (PI = $[\Sigma_{n \geq 1}(P_n/2^n)]/[\Sigma_{n \geq 0}(P_n/2^n)]$, n = cell doubling, p = % of cells in n). For cytokine treatment BMMCs were incubated with IL-6, IL-7 and IL-15 (Immunotools) for 20 hours.

Isolation of RNA and quantitative RT-PCR

RNA was isolated from purified $CD4^+$ T cells using the RNeasy Plus mini kit (QIAGEN). First-strand cDNA synthesis was performed using a Reverse Transcription system (Promega). Quantitative RT-PCR experiments were performed using the LightCycler 480 System (Roche Diagnostics), 2X SYBR Green 1 Master (Roche Diagnostics), and β-actin as housekeeping gene for relative quantification. Sequence-specific oligonucleotide primers were designed using Primer3 software and synthesized by MWG Biotech (Ebersberg, Germany).

Flow cytometry

Single-cell suspensions were stained with 5 μL TrueStain FcX (Biolegend) for 20min on ice to block Fc receptors. Surface staining was performed by adding a panel of Abs for 30min at 4°C. If necessary cells were fixed and permeabilized using the Cytofix/Cytoperm kit (BD) and incubated with intracellular Abs. Dead cells were excluded by Zombie Violet Fixable Viability Kit (Biolegend) or 7AAD (Miltenyi) staining. Labeled cells were measured using a FACSCanto II (BD Biosciences). Data were analyzed using Flowjo software.

FcμR expression: PBMCs were stained with rabbit α-FcμR for 30min at 4°C. Then the cells were washed and surface staining was performed together with secondary α-rabbit Alexa647. As control cells were stained without rabbit α-FcμR. The expression was calculated as ΔMFI = MFI of FcμR plus secondary α-rabbit Alexa647 – MFI of secondary α-rabbit Alexa647.

IgM binding: PBMCs were incubated with 47μg/ml IgM-Alexa488 or kept in serum free medium. After washing, surface staining was performed. The IgM binding was calculated as ΔMFI = MFI of IgM-Alexa488 – MFI of FMO control.

CD3 recycling: Control and IgM preincubated PBMCs were stimulated with 5μM PDBu for 1 hour at 37°C, washed at 4°C and transferred to 37°C for 10–60 min. Cells were shifted directly to ice and surface CD3 expression on $CD4^+$ T cells was measured at all time points by flow cytometry. PBMCs were also incubated at 37°C in the presence of 10μg/ml Cyclohexamide, 20ng/ml Actinomycin D or 1μM MG132 (all purchased from Sigma Aldrich). CD3 surface expression on $CD4^+$ T cells was measured by flow cytometry after 20 hours.

TCR internalization: PBMCs were incubated for 20 hours with 47μg/ml IgM or kept in serum-free medium. After washing, cells were activated with 1μg/ml mouse α-CD3 (OKT3; Biolegend) at 37°C for 10-240min. Then cells were shifted to ice and stained with donkey α-mouse Alexa488 and α-CD4-VioGreen (Miltenyi; REA623). Percent receptor downregulation was calculated as: 100x (MFI cells incubated with α-CD3 / MFI cells unstimulated on ice)

FcμR surface trafficking: PBMCs were treated for half an hour with 10μg/ml BFA, 20ng/ml actinomycin d or 1μM MG132 (all purchased from Sigma Aldrich) prior to α-FcμR Ab incubation for 20 hours. Alternatively 47μg/ml IgM was added together with α-FcμR

Ab. As control PBMCs were incubated for 30min at 4°C with rabbit α-FcμR Ab. After surface staining of $CD3^+CD4^+$ T cells, cells were fixed, permeabilized and stained with secondary α-rabbit Alexa647.

Cell Sorting

T cells were isolated from fresh PBMCs by magnetic cell sorting using the MACS human Pan T cell isolation kit (Miltenyi Biotech) following manufacturer's protocol. Purified T cells were then stained with α-CD3, α-CD4, α-CD8, α-CD45RA, and α-CCR7. Labeled cells were sorted with a FACSAria II flow cytometer (BD Biosciences). Cells were sorted into $CD4^+CCR7^+CD45RA^+$, $CD4^+CCR7^+CD45RA^-$ and $CD4^+CCR7^-CD45RA^-$ T cells. The cells were collected into RPMI 1640 medium containing 10% FCS and washed once prior RNA isolation. The purity of each subset was > 95% as determined by flow cytometry.

ImageStream

PBMCs were incubated in the presence or absence of IgM-Alexa488 using concentrations between 0.7μg/ml and 47μg/ml. After washing, cells were stained with α-CD4 PE and measured using ImageStream Mark II (MKII) Imaging Flow Cytometer system (Amnis). Cells were gated on aspect ratio versus bright field area to include only single cells, using the gradient root-mean-square feature to include cells in focus. Apoptotic cells were excluded from the analysis based on morphology. Cells in focus were gated for the expression of CD4 and IgM internalization was analyzed using IDEAS software.

Immunofluorescence analysis of tonsil biopsies

Formalin-fixed, paraffin-embedded 4-μm tonsil sections were deparaffinised in xylene and re-hydrated in ethanol. The slides were boiled in 0.01 M citrate buffer (pH 6) for 16 min in the microwave for epitope retrieval and allowed to cool for about 1 h at room temperature. After cooling the slides were washed twice with Aqua dest. and with TBS for 5min. Slides were blocked with 3% skim milk in TBS/Tween for 20 min at room temperature. Rabbit α-FcμR (Sigma Aldrich) and mouse α-CD3 were administered in TBS and incubated overnight at 4°C. After washing three times with TBS/Tween, the slides were incubated with α-mouse Alexa488, α-rabbit Cy3 and dapi for 1h at 4°C. The slides were washed three times with TBS/Tween and twice with TBS for 5min. Cell Voyager CV1000 microscope (Yokogawa-Bruker) were used to analyze stained slides.

Immunofluorescence confocal microscopy

FcμR mediated IgM uptake: Purified CD4+ T cells or PBMCs were incubated with 47μg/ml IgM-Alexa488 in presence of rabbit α-FcμR (Sigma Aldrich). Surface were stained with α-CD4-BV421 and cells fixed with BD cytoperm/cytofix buffer and washed with Perm/Wash buffer (BD). The cells were washed twice with PermWash buffer and PBS Cells and stained with α-rabbit Cy3 to visualize FcμR.

IgM colocalization in endosomes: PBMCs were incubated with 47μg/ml IgM Alexa488.The surface was stained with α-CD4-BV421 and cells were fixed with BD cytoperm/cytofix buffer and washed with Perm/Wash buffer (BD). Cells were stained with rabbit α-EEA1, α-Rab7 or α-Rab11 (Cell Signaling). After washing, α-rabbit Cy3 (Abcam) was used to visualize endosome marker.

FcμR surface trafficking: PBMCs were incubated for 30min at 4°C in the presence of rabbit α-FcμR (Sigma Aldrich), then washed and shifted for 20 hours to 37°C. Additionally cells were incubated for twenty hours at 37°C in the presence of α-FcμR Ab. The surface was stained with α-CD4-BV421 and cells were fixed with BD cytoperm/cytofix buffer, washed with Perm/Wash buffer and stained with α-rabbit Cy3 to visualize FcμR which had been expressed on the surface during incubation time in the presence of rabbit α-FcμR Ab.

After the last incubation step, cells were resuspended in 100μl PBS, transferred to coverslips by cytospin and mounted with fluorescent mounting medium (Dako). Images were acquired on Cell Voyager CV1000 (Yokogawa-Bruker).

ELISA assay

Purified $CD4^+$ T cells were seeded at a density of 1×10^6 cells and incubated with 47μg/ml IgM for 20h or kept untreated in serum-free medium. Supernatants were collected after six, twelve, twenty-four and forty-eight hours after transfer to plates coated with 1μg/ml α-CD3 and 1μg/ml soluble α-CD28 was added to some wells. IFNγ was assessed in supernatants using Elisa kits (Biolegend)

Western blot

$CD4^+$ T cells were isolated from PBMCs by negative selection with MACS and preincubated for 20 hours with 47μg/ml IgM or kept in serum-free medium. After preincubation, T cells were transferred to plates coated with 1μg/ml α-CD3 and 1μg/ml soluble α-CD28 was added. Cells were lysed in ice-cold lysis buffer [5mM NaP2P, 5mM NaF, 5mM Na3VO4, 5mM EDTA, 150mM NaCl, 50mM Tris (pH 7.3), 1% NP-40, aprotinin and leupeptin (50 μg/ml each)] and centrifuged at 15000xg for 15 min at 4°C. Cell lysates were electrophoresed on a NuPAGE gel (Invitrogen) and transferred onto a polyvinylidene difluoride (PVDF) membrane (Millipore) by semi-dry blotting (100mA, 90 min). The primary antibodies were diluted in tris-buffered saline containing 0.5% Tween-20 and either with 5% nonfat dry milk or with 5% bovine serum albumin (BSA) for phospho antibodies. Peroxidase-conjungated antibodies (Pierce) served as secondary reagents (1:5000). Enhanced chemiluminescence was used for antigen detection (Super Signal, Thermo Fischer). As a loading control for whole cell lysates β-actin (Santa Cruz Biotechnology,sc-1615) was applied. Protein lysates were subjected to immunoblotting with antibodies against phospo-IκBα (Ser32), clone 14D4 (Cell signaling, #2859), pan IκBα (Cell

signaling, #9242), phospho-ERK1/2 (Thr202/Tyr204) (Cell signaling, #9101) and pan ERK1/2 (Cell signaling, #9102). Blot pixel densities were quantified using ImageJ (NIH) and normalized to actin (Schindelin et al., 2012).

QUANTIFICATION AND STATISTICAL ANALYSIS

All data are shown as mean ± standard error of the mean (SEM). Statistical analysis was performed using GraphPad Prism software version 5.0 (GraphPad Software). To determine the significance of differences between two groups, the Wilcoxon matched pairs test, the unpaired Mann-Whitney test and two way ANOVA test were used, as indicated in the figure legends. For correlations, statistical significance was assessed by Spearman correlation analysis. A p value less than 0.05 was considered significant, except in the assessment of the age-related differences in the *FCMR* methylation sites between young and elderly, a more stringent p value threshold ($p < 0.001$) was used.